

CuO nanoflowers as an electrochemical pH sensor and the effect of pH on the growth

Siama Zaman, Muhammad Asif, A. Zainelabdin, Gul Amin,
Omer Nur and Magnus Willander

Linköping University Post Print

N.B.: When citing this work, cite the original article.

Original Publication:

Siama Zaman, Muhammad Asif, A. Zainelabdin, Gul Amin, Omer Nur and Magnus Willander, CuO nanoflowers as an electrochemical pH sensor and the effect of pH on the growth, 2011, JOURNAL OF ELECTROANALYTICAL CHEMISTRY, (662), 2, 421-425.

<http://dx.doi.org/10.1016/j.jelechem.2011.09.015>

Copyright: Elsevier

<http://www.elsevier.com/>

Postprint available at: Linköping University Electronic Press

<http://urn.kb.se/resolve?urn=urn:nbn:se:liu:diva-73334>

CuO nanoflowers as an electrochemical pH sensor and the effect of pH on the growth

S. Zaman*, M. H. Asif, A. Zainelabadin, G. Amin, O. Nur and M. Willander

Department of Science and Technology, Campus Norrköping,

Linköping University, SE-60174 Norrköping, Sweden

***Corresponding Author:** saiza@itn.liu.se

Abstract

Well-crystallized flower-shaped copper oxide nanostructures composed of thin leaves have been synthesized by simple low-temperature chemical bath method and used to fabricate pH sensors. We examined the effect of the pH on the growth of the CuO nanostructures. By changing the pH of the precursor solution different morphologies of the CuO nanostructures were obtained. CuO nanoflowers have recently become important as a material that provides an effective surface for electrochemical activities with enhanced sensing characteristics. The proposed sensor exhibited a linear electrochemical response within a wide pH range of (2-11). The experimental results (time response, electrochemical activity, reproducibility, absorption spectra, and XRD) indicate that the CuO nanoflowers can be used in pH sensor applications with enhanced properties.

Keywords: CuO nanoflower, morphological effect, electrochemical, pH sensor, repeatability.

1. Introduction

The monitoring of the pH is extensively required in laboratories, clinics and industries, as many chemical processes are pH dependent. Therefore fast, accurate and reliable pH measurements are important in many applications [1, 2]. There are many different pH measurement techniques and the most common approaches that exploit oxides as pH-sensitive layers are the potentiometric [3], ion sensitive field effect transistors [4], and conductometric / capacitive [5]. In these techniques potentiometric approach is mostly used because it is less complex in fabrication and has been used over a longer period.

Cupric oxide (CuO) is an important p-type metal oxide semiconductor with narrow bandgap (1.2 eV), and has been investigated as an attractive material due to its plentiful unique characteristics [6- 8]. The synthesis of the CuO nanostructures is very important for several applications [9- 13]. The pH of the solution is very important parameter for growth of CuO nanostructures, and by varying the pH various shapes were obtained [14, 15]. CuO nanostructures have unique advantages including high specific surface area, chemical stability, electrochemical activity, and high electron communication features [16]. Owing to its exceptional electrochemical activity and the possibility of promoting electron transfer at a low potential, nanostructured CuO is a good candidate for sensing application [17- 22].

In this letter we report the fabrication of newly developed CuO nanoflowers (NFs) pH sensors. The effect of the pH on growth morphology of the CuO nanostructures was studied by changing the pH of the solution. The fabricated pH sensor shows a linear response for the electrochemical potential difference for a large dynamic range of pH (2 - 11). It exhibited good potential stability and fast time response. Moreover the developed sensors can work efficiently in small volumes.

2. Experimental details

The CuO NFs were grown on the glass substrate. For the synthesis of CuO NFs, 5mM of copper nitrate and 1mM of hexamethylene tetramine (HMT) were mixed in de-ionized (DI) water in a glass vessel. The solution was magnetically stirred for 5 min. Then the reaction vessel containing the substrate was loaded in a laboratory oven at 90 °C for 4 to 5 hrs. To check the role of the pH on the growth of CuO, the pH of the solution was adjusted from 2 to 11 pH by adding HNO₃ or NH₃.H₂O. The morphology and the structural properties of the as grown CuO nanoflowers were investigated by field emission scanning electron microscopy (FE-SEM; JEOL, JSM-6335F) and high resolution transmission electron microscope (HRTEM). The powder X-ray diffraction (XRD) was also measured with an X-ray diffractometer equipped with Cu K α 1 radiation.

The electrochemical measurements were conducted using two electrode configurations, consisting of CuO NFs as a working electrode and Ag/AgCl as a reference electrode. The response of the electrochemical potential difference of the CuO NFs versus an Ag/AgCl reference electrode to the changes in the buffer was measured for pH ranging from 2 to 11 at room temperature. Three set of samples fabricated identically for pH sensors to check the repeatability and reproducibility.

3. Results and Discussion

3.1 The morphology and structure of CuO NFs

FESEM image reveals the general morphology of CuO nanoflowers (NFs) structure. Figure.1a depicted the plan view of the CuO NFs, which uniformly covered the substrate. Inset

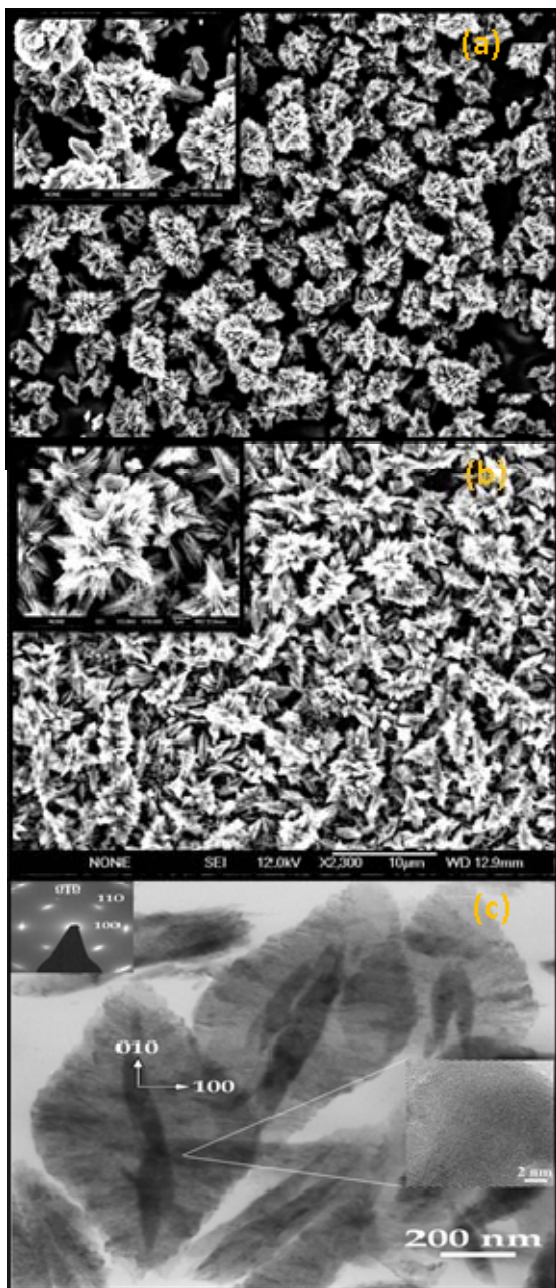


Figure 1: (a) Field emission scanning electron microscope image of CuO NFs before pH measurements. (b) After pH measurements from pH= 2 to pH= 11. (c) TEM image of as grown CuO NFs and inset is the SAED pattern of structure.

in Fig. 1a shows the enlarged view of the CuO NFs and as can be seen each nanoflower composed of a several layers of leaf like structure. The size of the nanoleaves is different in the bottom and top surface of the nanoflower. They have a wider base with a very sharp tip and narrow at the centre of the flower. The solubility of the developed sensors was examined very carefully by monitoring the FESEM image of the sample after exposure to the electrolyte for each buffer under various pH values. Fig. 1b shows the influence of the pH environment on the CuO NFs, as clearly seen very small part of the NF has been etched after it was subjected to different pH solution. TEM images of a single CuO nanoleaf which accumulate to form the NFs is shown in Fig. 1c and the inset shows the HRTEM image. Figure 1c shows that the CuO single leaf have well defined structure. The growth of the CuO nanoleaf along the (010) planes is faster compared to the (100) plane. As reported in the literature [23] among the three planes (001), (010) and (100), the most thermodynamically stable plane is the (001) while the least stable one is (010) due to the highest and lowest density of copper atoms on these planes. Therefore, preferential aggregated growth takes place along the (010) which has the highest reactivity. The inset of Fig. 1c, i.e the selected area electron diffraction (SAED) pattern shows that the CuO nanoleaves have good polycrystalline structure.

X ray diffraction pattern of CuO NFs shows the growth orientation and crystallinity of the structure. The XRD peaks indexed in Fig. 2 are consistent with the JCPDS (card no. 05-661) and ascribed a phase of pure monoclinic CuO crystal, however no other impurity peak was observed.

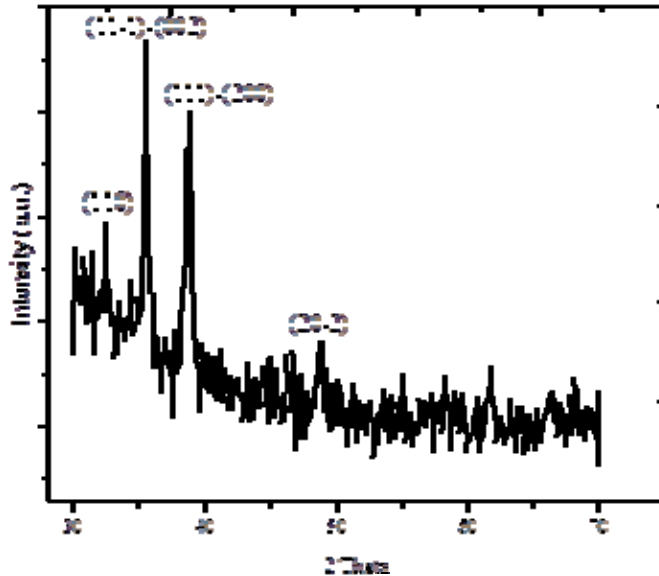


Figure 2: X ray diffraction pattern of CuO NFs at room temperature.

3.2 Effect of pH on the morphology of CuO

To study the effect of the pH on the morphology of the nanoflowers, we adjusted the pH from 2 to 11, under inherent pH value flower like structure was obtained. $\text{NH}_3 \cdot \text{H}_2\text{O}$ was added to adjust the pH of the precursor solution from 7 to 11. CuO petals were obtained at pH = 7, and by increasing the pH to 8, 9 and 10 the diameter of the petals were observed to shrink, as shown in Fig 3b, c, d and e. The CuO nanostructures obtained at pH = 11 strikingly different from those obtained at lower pH, in which a tiny petals merge together to form an aloe vera (AV) like CuO NFs with ultra sharp branches. The reaction mechanism involved in the formation of these nanostructures can be summarized as follow

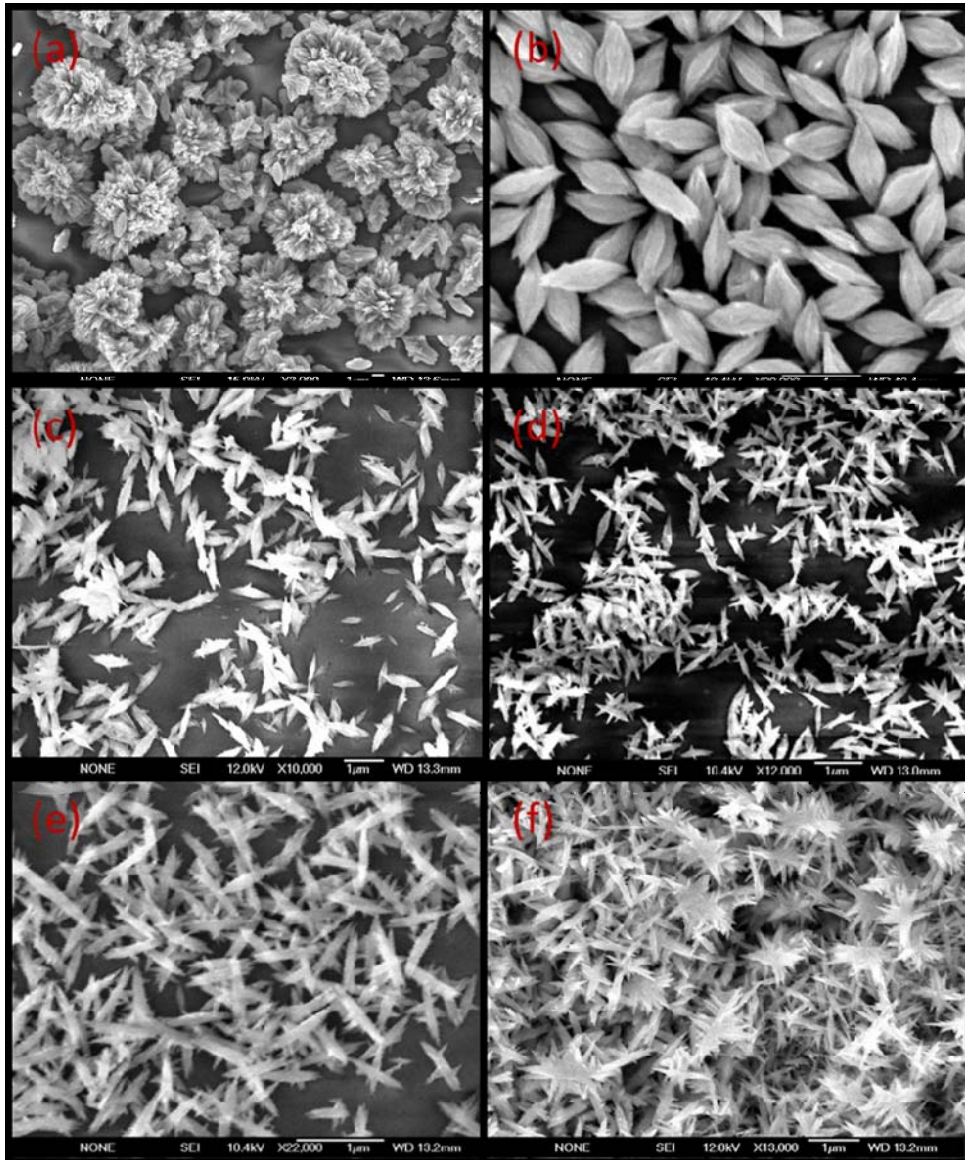
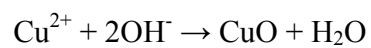
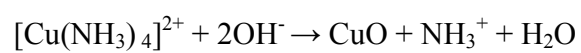
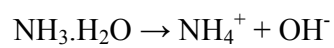


Figure 3: FESEM of CuO nanostructures grown under different pH solution at (a) inherent pH 6.5 (b) pH= 7 (c) pH= 8 (d) pH= 9 (e) pH= 10 (f) pH= 11.



At the initial stage of the reaction, a small amount of CuO nuclei was formed in the solution. The surface of these nuclei is either negatively or positively charged, surface will attract the opposite charge (OH^- or Cu^{2+}) to it, and a new surface covered with ions will in turn attract ions with opposite charges to cover the next surface. Thus CuO nanostructures are formed after the aggregation is completed. The morphology of the CuO nanostructures can be affected by the OH^- concentration in the solution, and it is suggested that the growth of CuO nanostructures was highly effected by chemical potential of the OH^- ions, and the chemical potential of the OH^- is determined by the pH value. The concentration of the OH^- in the solution is low without adding $\text{NH}_3\cdot\text{H}_2\text{O}$ in the precursor solution. A small amount of OH^- has a weak interference on Cu^{2+} moving to nuclei, this gives a chance for nuclei random aggregation, and the next step is that CuO crystal grains starts to grow on these nuclei, which are beneficial for the formation of a flower-like structure, as shown in Fig. 3a. When the $\text{NH}_3\cdot\text{H}_2\text{O}$ which is an alkali was added, more OH^- may neutralize positive charges in the surface of the CuO, and therefore affect the aggregation [24]. Thus, the CuO nuclei grow slowly and orderly on the previous nuclei, which are beneficial for the formation of only petals like structures, as shown in Fig. 3b. At higher pH = 11, the OH^- concentration is increased and will enhances the growth on specific crystal face of the structures, and side branches of petals are grow rapidly and form a AV like structure. One possible reason may be due to the higher OH^- concentration which creates diffusion layers on certain surfaces of the CuO nanostructures. This may produce additional anisotropy, allowing only energetically favorable crystallographic planes to grow [25]. The other possible reason is the electrostatic attraction between the individual CuO petals resulting in strong binding between them [26]. At lower pH we did not get any growth at this specific time, and this may be due to less OH^- in the solution. At this low concentration of OH^- , CuO nuclei will not be formed.

3.3 Electrochemical measurements

The electrochemical pH response of the CuO nanoflowers in Fig. 4a indicates excellent linearity and repeatability. The potential difference (electromotive force emf) between the CuO NFs working electrode and reference (Ag/AgCl) electrode changes within a wide range of pH from 2 to 11. The actual electrochemical potential cell can be described by the diagram below:



The change in the emf was attributed to the different pH buffer solution via a calibration procedure which shows good linearity with a sensitivity 28mV/decade and a correlation coefficient r^2 values of about 0.953 which is calculated from near-Nernstian response. A Nernstian response of an anhydrous CuO film to pH changes is described by the following redox reaction [27];



To check the output response, stability, and repeatability of the electrode, the sample was tested three to four times in an PBS buffer saline with pH ranging from 2 to 11, the result is shown in Fig. 4b. It was observed that the CuO NFs showed stable potentiometric response, excellent reproducibility, and good sensor stability. Figure 4c shows the output voltage versus time for the fabricated working electrode at a specific pH. The fabricated electrochemical sensor is repeatable and stable with time to reach a stable signal of around 25 seconds of detection which shows relatively fast electrochemical reaction between the CuO NFS and the pH but slightly lower than the other pH sensors. This may be due to the reason that the response time is mostly affected by the porous properties of the sensing material. The buffer pH solution needs to

accumulate in the liquid in the pores of the CuO NFs in which the pores increases the response time [28]. Since the CuO NFs sensors are porous, so the sensor response is slightly slower.

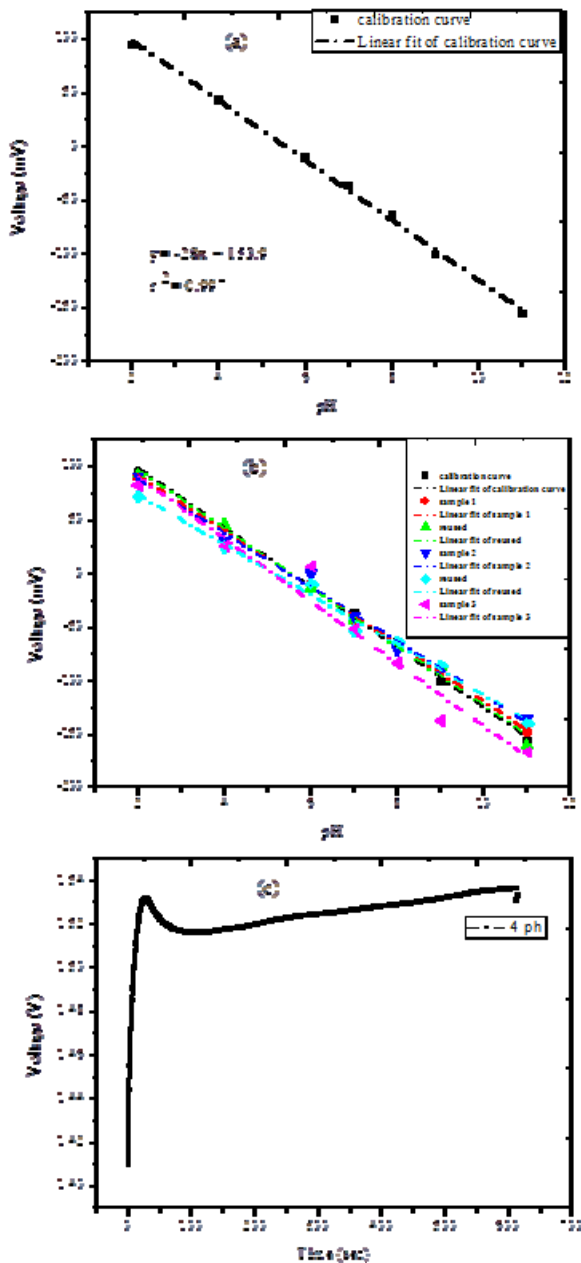


Figure 4: (a) Calibration curves of the CuO NFs pH electrode in pH buffer solution (b) Repeatability and reproducibility test of three CuO NFs pH sensor electrodes at various pH buffer solutions. (c) Output voltage response as a function of time showing good stability.

After the potentiometric measurements, the sample was checked using the amperometric electrochemical technique. The output signal was linearly dependent on the pH range from 2-11 when applying a constant bias potential of 0.1 V. Hence the interaction between the CuO NFs and the pH buffer solution generated an amperometric output signal. The current is changed when the pH buffer solution is modified. Figure 5 depicts the calibration curve of the current versus pH.

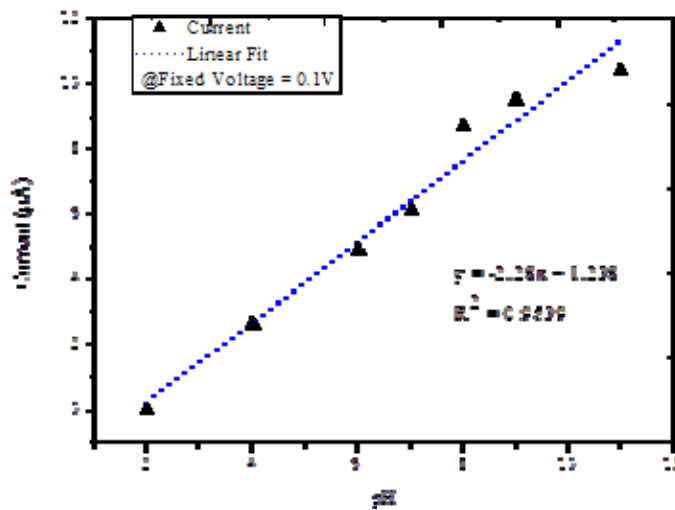
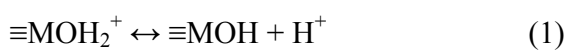


Figure 5: Calibration curve for current response versus pH buffer solution varying from pH 2 to 11 at accumulated voltage 0.1 V.

There is different pH sensing mechanism theories for metal oxide nanostructures pH sensors. Surface chemistry of metal oxide tends to control their charging behavior. In water, surface chemistry of hydrous metallic oxides develops through protonation–deprotonation of water molecules bonded to surface metal ions (Eqs. (1) and (2)):





(where M stands for the metal ion and $\equiv\text{MOH}$ represents the amphoteric electroneutral surface groups at surface sites, accounting for the $\equiv\text{M}$ ability to exchange ligands). The pH dependent charge of an oxide thus results from the speciation of hydroxyl surface groups and the proton transfer at the surface. The portion of the surface charge attributable to specific interactions with OH^- and H^+ ions corresponds to the difference between protonated and deprotonated $\equiv\text{MOH}$ groups [29].

In acid solution, it is known that for the hydrogen oxidation at a hydrogen electrode, the electrode potential increases with rising pH. Protons are released by the dissociative adsorption of water and superacid OH groups. In alkaline solution, it is known that for the oxygen reduction at an oxygen electrode, the electrode potential decreases with rising pH. By the dissociative adsorption of water, hydroxide sites are formed and they are bound [27].

The important parameter for the ion-sensitive layers is the density of surface sites that form the pH-dependent surface potential. CuO NFs as a pH sensor is based on the activity of the electrolyte-NFs/interface, in which the H^+ specific bonding sites existing at the CuO surface can hydrogenate after contact with the electrolyte solution. This sites can protonate or deprotonate, leading to a surface charge and a surface potential that is dependent on the electrolyte pH.

A Helmholtz layer is developed by the adsorption of the ions or the molecules on the CuO surface, by oriented dipoles, or by the formation of surface bonds between the solid surface and species in the solution [30, 31].

4. Conclusions

In conclusion, different CuO nanostructures were obtained under different pH in the growth solution. By increasing the pH of the solution, more OH^- is generated which is mainly

responsible to change the morphology of the CuO structures. CuO NFs based pH sensor electrodes were fabricated to check the sensitivity of the CuO NFs for the pH in the range 2 to 11. The potentiometric response of this pH sensor appeared linear in a pH range between 2 and 11. The fabricated sensor demonstrated good repeatability and reproducibility. This experiment paves the way for CuO nanostructures to find applications in biological fluids.

References

- [1] H. Galster, pH Measurements—Fundamentals, Methods, Applications, Instruments, VCH Publishers, New York, (1991).
- [2] W. Göpel, T. A. Jones, M. Kleit, I. Lundströ, T. Seiyama Sensors—a comprehensive survey. VCH, New York (1991).
- [3] B. Lakard, O. Segut, S. Lakard, G. Herlem, T. Gharbi, Sensors and Actuators B 122 (2007) 101-108.
- [4] Y. Liu, T. Cui, Sens. Actuators B Chem 123 (2007) 148-152.
- [5] E. Gill, K. Arshak, A. Arshak, O. Korostynska, Microsyst Technol 14 (2008) 499-507.
- [6] M. Yin, C. K. Wu, Y. B. Lou, C. Burda, J. T. Koberstein, Y. M. Zhu, S. O'Brien, J. Am. Chem. Soc. 127 (2005) 9506-9511.
- [7] K. Zhou, R. Wang, B. Xu, Y. Li, Nanotechnology 17 (2006) 3939-3943.
- [8] Y. Xu, D. Chen, X. J. Jiao, Phys. Chem. B 109 (2005) 13561-13566.
- [9] M. Cao, C. Hu, Y. Wang, Y. Guo, C. Guo, E. Wang, Chem. Commun. (2003) 1884-1885.
- [10] X. C. Jiang, T. Herricks, Y. N. Xia, Nano Lett. 2 (2002) 1333-1338.
- [11] W. Z. Wang, Y. J. Zhan, G. H. Wang, Chem. Commun. (2001) 727-728.
- [12] X. J. Zhang, G. F. Wang, X. W. Liu, J. J. Wu, M. Li, J. Gu, B. Fang, J. Phys. Chem. C 112 (2008) 16845-16849.
- [13] B. Liu, H. C. Zeng, J. Am. Chem. Soc. 126 (2004) 8124-8125.
- [14] J-H. Pee, D-W. Lee, U-S. Kim, E-S. Choi, Materials Science Forum 534 (2007) 77-81.
- [15] J. Y. Xiang, J. P. Tu, L. Zhang, Y. Zhou, X. L. Wang, S. J. Shi, Journal of Power Sources 195 (2010) 313–319.

- [16] W. Jia, M. Guo, Z. Zheng, T. Yu, Y. Wang, E. G. Rodriguez, Y. Lei, *Electroanalysis* 20 (2008) 2153-2157.
- [17] Y. Li, Y. Wei, G. Shi, Y. Xian, L. Jin *Electroanalysis* 23 (2011) 497-502.
- [18] W. Z. Jia, M. Guo, Z. Zheng, T. Yu, Y. Wang, E. G. Rodriguez, Y. Lei, *Electroanalysis* 20 (2008) 215-2157.
- [19] E. Reitz, W. Z. Jia, M. Gentile, Y. Wang, Y. Lei, *Electroanalysis* 20 (2008) 2482-2486.
- [20] Z. J. Zhuang, X. D. Su, H. Y. Yuan, Q. Sun, D. Xiao, M. M. F. Choi, *Analyst* 133 (2008) 126-132.
- [21] X. J. Zhang, G. F. Wang, W. Zhang, N. J. Hu, H. Q. Wu, B. Fang, *J. Phys. Chem. C* 112 (2008) 8856-8862.
- [22] X. J. Zhang, A. X. Gu, G. F. Wang, Y. Wei, W. Wang, H. Q. Wu, B. Fang, *Cryst Eng Comm.* 12 (2010) 1120-1126.
- [23] Z. Zhang, H. Sun, X. Shao, D. Li, H. Yu, M. Han, *Adv. Mater.* 17 (2005) 42-47.
- [24] H. Zhang, J. Feng, M. Zhang, *Materials Research Bulletin* 43 (2008) 3221-3226.
- [25] J. Liu, X. Huang, Y. Li, K. M. Sulieman, X. He, F. Sun, *Crystal Growth & Design* 6 (2006) 1690-1696.
- [26] M. Vaseem, A. Umar, S. H. Kim, Y-B. Hahn, *J. Phys. Chem. C* 112 (2008) 5729-5735.
- [27] P. Kurzweil, *Sensors* 9 (2009) 4955-4985.
- [28] W. D. Huang, H. Cao, S. Deb, M. Chiao, J. C. Chiao, *Sensors and Actuators A* 169 (2011) 1-11.
- [29] M. Guedes, J. M. F. Ferreira, A. C. Ferro, *Journal of Colloid and Interface Science* 330 (2009) 119-124.
- [30] S. Al-Hilli, M. Willander, *Sensors* 9 (2009) 7445-7480.
- [31] M. Green, *J. Chem. Phys.* 31 (1959) 200-203.

